Analytical Theory of Thin-Film Schottky Diodes

DOI:
10.1021/acsaelm.9b00324

Document Version
Accepted author manuscript

Analytical Theory of Thin-Film Schottky Diodes

Joshua Wilson,[†] Jiawei Zhang,[†] and Aimin Song[*,†,‡]

[†]*School of Electrical and Electronic Engineering, University of Manchester, Manchester, M13 9PL, United Kingdom*

[‡]*Center of Nanoelectronics and Microelectronics, Shandong University, Jinan 250100, People's Republic of China*

E-mail: a.song@manchester.ac.uk

Abstract

Thin-film electronics straddles the border between bulk electronics and the quantum realm. Though thin-film devices are increasingly prevalent, our understanding of their operation remains incomplete. Recent research has highlighted inconsistencies between the established theory and practical operation of thin-film Schottky junctions, a key constituent of many electronic devices. In thin-film devices, the entire semiconductor film can be depleted; thus, the standard depletion approximation no longer holds as the boundary conditions of Poisson's equation are changed. The effects of these changes upon the current through the Schottky diode were investigated using both analytical theory and device simulations, with particular focus on the dependence of the reverse current upon semiconductor thickness. As thin-film electronics is increasingly geared towards the use of disordered materials and low-cost processing, it is of foremost importance to develop a theory of inhomogeneous thin-film Schottky junctions. A model was devised for a thin-film Schottky diode with a single inhomogeneity in the barrier height. Analytical theory and device simulations based upon this model were found to be in

agreement about the thickness dependence of the effective barrier height in thin-film Schottky diodes with inhomogeneous barrier heights. Analytical theories were derived for both thermionic emission and diffusion currents and demonstrated good agreement with the results of device simulations. Finally, as practical devices contain a distribution of barrier heights, a multiple barrier height model for thin film Schottky diodes was derived and used to fit an experimental result. Our results offer practical insight for device design, not just for Schottky diodes, but also for p-n junctions, organic light-emitting diodes and other heterostructure devices.

Keywords

Schottky Diodes, Metal-Semiconductor Junctions, Inhomogeneities, Thin-Film Electronics

1 Introduction

Thin-film electronics has the potential to revolutionise the way that people interact with their environment, bringing greater connectivity and new devices for healthcare and leisure. However, a full realisation of this vision will rely upon establishing a solid theoretical understanding of the characteristics of thin-film components. Research into thin-film transistors (TFTs) has a long history and the factors affecting their behaviour, such as short-channel effects,[1–4] are well-documented. Though Schottky junctions are also an essential, and thoroughly researched,[5] constituent of solid-state devices, investigations into the behaviour of thin-film Schottky diodes are more limited. Schottky junctions in thin-film devices do not necessarily conform to the theory of a metal-semiconductor junction as proposed by Schottky.[6,7] For example, in thin-film technology, Schottky diodes can be fully depleted.[8] Furthermore, as thin-film electronics is likely to employ disordered materials (e.g. indium gallium zinc oxide and organic semiconductors) and less rigid processing techniques (e.g. printing) the resulting Schottky junctions will contain significant disorder. Currently, there is no established theory

for thin-film Schottky diodes with an inhomogeneous Schottky junction and many papers[9,10] evaluate the behaviour of thin-film diodes using either Tung's model,[11] which assumes the depletion width is smaller than the thickness of the diode, or the model proposed by Werner and Güttler,[12] which ignores the two-dimensional effects of interface disorder and so fails to capture the true device behaviour. It was recently discovered that the combination of thin semiconductor layers and disorder at the Schottky interface produces behaviour in thin-film Schottky diodes[13] and source-gated transistors[14] which cannot be explained by the aforementioned theories. Such inconsistencies between device theory and behaviour demand a carefully considered resolution.

This work develops an analytical theory of thin-film Schottky diode behaviour. By studying the potential inside the semiconductor, theories for thermionic emission and diffusion are derived and compared with the results of device simulations. Analytical models are also developed to incorporate barrier height inhomogeneities and the behaviour of these models is compared to device simulations. Particular attention is paid to the reverse bias behaviour, which is little studied, but often the limiting factor in rectification ratio and can be dramatically affected by the semiconductor thickness.

2 Device Simulations

To check the validity of the analytical theories developed in this work, thin-film Schottky diodes were simulated in Silvaco Atlas (version 5.14.0.R). The basic structure of the Schottky diodes considered in this work is shown in Fig. 1. The modelled diodes are made up of a three-layered structure with a semiconductor, in this case indium gallium zinc oxide (IGZO), sandwiched between an ohmic contact (bottom) and a Schottky contact (top). The interface between the Schottky contact and the IGZO is at $z = 0$, the interface between the ohmic contact and the IGZO is at $z = H$ and the centre of the diode is at $x = 0$. The model assumes a symmetry in the y-direction and has a depth, L_y. The total width of the

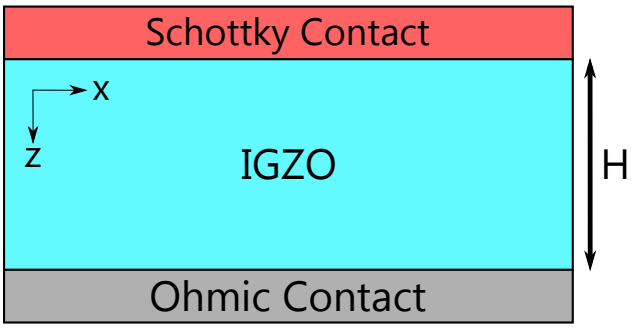

Figure 1: Structure of the Schottky diode model with a homogeneous barrier height.

diode, L_x, is 100 nm. The simulation parameters used to model IGZO are based on the parameters outlined by Fung *et al.*[15,16] The mesh density within the IGZO layer was fixed for all thicknesses and was denser near the Schottky interface in order to resolve finer detail.

3 Results and Discussion

3.1 Potential in a Fully-Depleted Thin-Film Schottky Diode

The electrostatic potential, ϕ, in a Schottky diode can be found using Poisson's equation

$$\nabla^2\phi = -\frac{qN_D}{\epsilon_0\epsilon_s}, \tag{1}$$

where N_D is the donor concentration, ϵ_0 is the permittivity of free space and ϵ_s is the relative permittivity. In thin-film Schottky diodes, such as the one in Fig. 1, the semiconductor layer may be fully depleted resulting in the following the boundary conditions:

$$\phi(0) = -\phi_B \tag{2}$$

and

$$\phi(H) = -(\phi_n + V), \tag{3}$$

where ϕ_B is the Schottky barrier height potential, H is the semiconductor thickness, ϕ_n is the Fermi potential from the conduction band edge, i.e. $-(E_C - E_F)/q$, and V is the applied bias. In a practical device the boundary conditions may be slightly different from the model proposed here as a result of interface states, doping from the metal contact or other factors. Thus, careful consideration of the boundary conditions will have to be made on a case by case basis, for example, by using capacitance-voltage measurements to obtain the effective thickness and the doping profile.

Solving Poisson's equation gives the potential in the semiconductor

$$\phi(z) = -\phi_B - \frac{qN_D}{2\epsilon_0\epsilon_s}z^2 + \left(\frac{\phi_{bi} - V}{H} + \frac{qN_D}{2\epsilon_0\epsilon_s}H\right)z, \tag{4}$$

where $\phi_{bi} = \phi_B - \phi_n$ is the built-in potential. As a result, the conduction band minimum is given by

$$E_C(z) = q\phi_B + \frac{q^2N_D}{2\epsilon_0\epsilon_s}z^2 - \left(\frac{q(\phi_{bi} - V)}{H} + \frac{q^2N_D}{2\epsilon_0\epsilon_s}H\right)z. \tag{5}$$

Figure 2a displays the conduction band minimum for 50 nm thick Schottky diodes with N_D varying from 10^{13} to 10^{17} cm^{-3} and applied biases of 0, -0.5 and -1 V. These plots show that E_C is dominated by its linear component and the quadratic term in Eq. 5 is comparatively weak. The dominance of the linear component for small H is to be expected, as z is very small. However, as H tends to W_D (the depletion width of a standard Schottky junction) the dominance of the linear term should wane because the thin-film model of E_C tends to the parabolic depletion approximation originally derived by Schottky.[6] Figure 2b shows that the analytical expression for E_C in Eq. 5 fits the simulation results for E_C for different thicknesses of semiconductor when $H < W_D$.

By differentiating Eq. 5, the electric field in the semiconductor is obtained:

$$\mathcal{E}(z) = \frac{qN_D}{\epsilon_0\epsilon_s}z - \frac{\phi_{bi} - V}{H} - \frac{qN_D}{2\epsilon_0\epsilon_s}H. \tag{6}$$

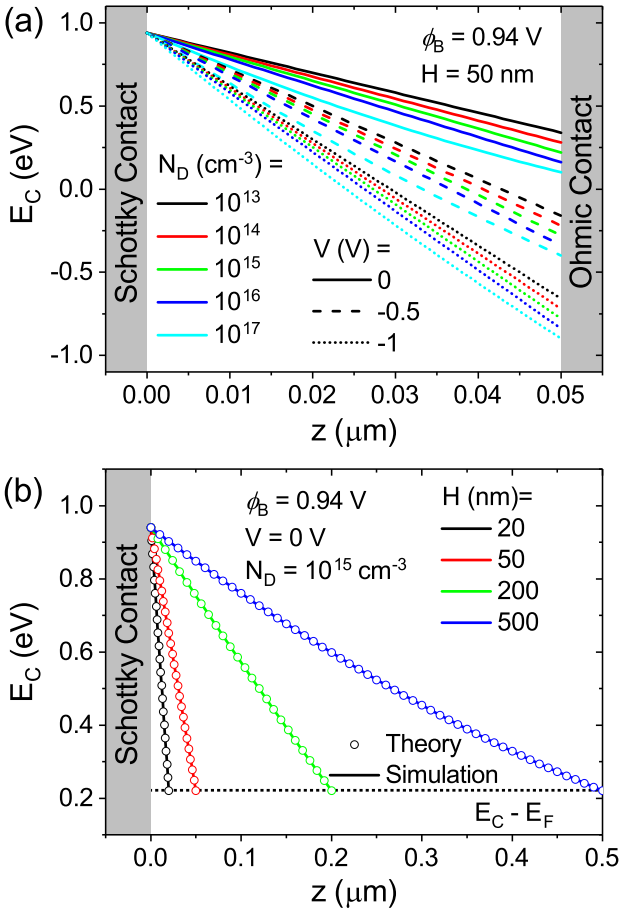

Figure 2: Conduction band minimum, E_C, in a fully depleted IGZO Schottky diode. (a) Calculated effects of varying doping and applied bias upon E_C in a 50 nm thick diode. (b) Comparison of theory and simulation of E_C for different thicknesses.

The value of the electric field at the Schottky junction is given by

$$\mathcal{E}(0) = -\frac{\phi_{bi} - V}{H} - \frac{qN_D}{2\epsilon_0\epsilon_s}H \tag{7}$$

and the magnitude of the maximum electric field in a fully depleted Schottky diode, $\mathcal{E}_{MT}$, can be defined as:

$$|\mathcal{E}(0)| = \mathcal{E}_{MT} = \frac{\phi_{bi} - V}{H} + \frac{qN_D}{2\epsilon_0\epsilon_s}H. \tag{8}$$

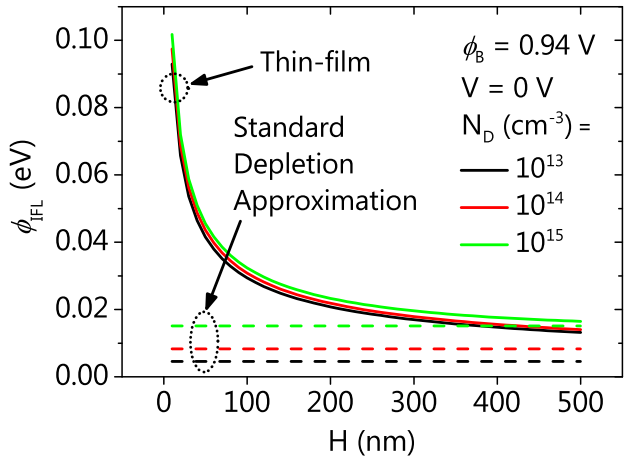

Figure 3: Image force lowering for different semiconductor thicknesses and carrier concentrations in both fully depleted Schottky diodes (solid) and Schottky diodes conforming to the standard depletion approximation (dashed).

3.1.1 Image Force Lowering

The electric field has a direct effect upon the Schottky barrier height as a result of image force lowering (IFL).[6] In a fully depleted thin-film Schottky diode, the potential barrier lowering due to IFL can be expressed as

$$\begin{aligned}\phi_{IFL} &= \sqrt{\frac{q\mathcal{E}_{MT}}{4\pi\epsilon_0\epsilon_s}} \\ &= \sqrt{\frac{q}{4\pi\epsilon_0\epsilon_s}\left(\frac{\phi_{bi}-V}{H}+\frac{qN_D}{2\epsilon_0\epsilon_s}H\right)}.\end{aligned} \tag{9}$$

Hence, the image force lowering of the barrier increases as H gets smaller, as shown in Fig 3, unlike the thickness-independent value predicted by the standard depletion approximation, defined as:[7]

$$\phi^*_{IFL} = \left[\frac{q^3N_D}{8\pi^2\epsilon_0^3\epsilon_s^3}\left(\phi_{bi}-V-\frac{kT}{q}\right)\right]^{1/4}. \tag{10}$$

For example, in the 100 nm thick diodes the barrier lowering can be more than a factor of six larger than the value predicted by the standard depletion approximation.

3.2 Current Transport in Fully Depleted Thin-Film Schottky Diodes

There are several different mechanisms for transport across a Schottky barrier. The dominant current limiting mechanism is dependent on factors such as the materials used to form the junction, the device geometry, the applied bias and the temperature. In the following sections image force lowering and quantum mechanical tunnelling are ignored for the sake of simplicity. The effects of IFL are discussed in the previous section and to incorporate the effects of tunnelling an additional barrier lowering factor proportional to the electric field can be subtracted from the potential profile.[17] In extreme cases, interface roughness and even the atomistic nature of the metal contacts may play a role, but the complexity such issues means that they defy simple analytical explanation.

3.2.1 Thermionic Emission Current

Considering the current density from thermionic emission without IFL is expressed as

$$J = A^* T^2 \exp\left(-\frac{q\phi_B}{kT}\right)\left[\exp\left(\frac{qV}{kT}\right) - 1\right], \tag{11}$$

it is clear that none of the parameters are affected by the changes to the shape of the barrier outlined in Section 3.1. Thus, the thermionic emission current in a fully depleted diode should be the same as predicted for the standard depletion approximation, though some exceptions will be discussed in Section 3.3.

3.2.2 Diffusion Current

When considering a diffusion-limited current, the differences between thin-film and bulk semiconductors do have an effect. The current density across the barrier can be expressed as

$$J \approx q\mu_n N_C \mathcal{E}_{MT} \exp\left(-\frac{q\phi_B}{kT}\right)\left[\exp\left(\frac{qV}{kT}\right) - 1\right]. \tag{12}$$

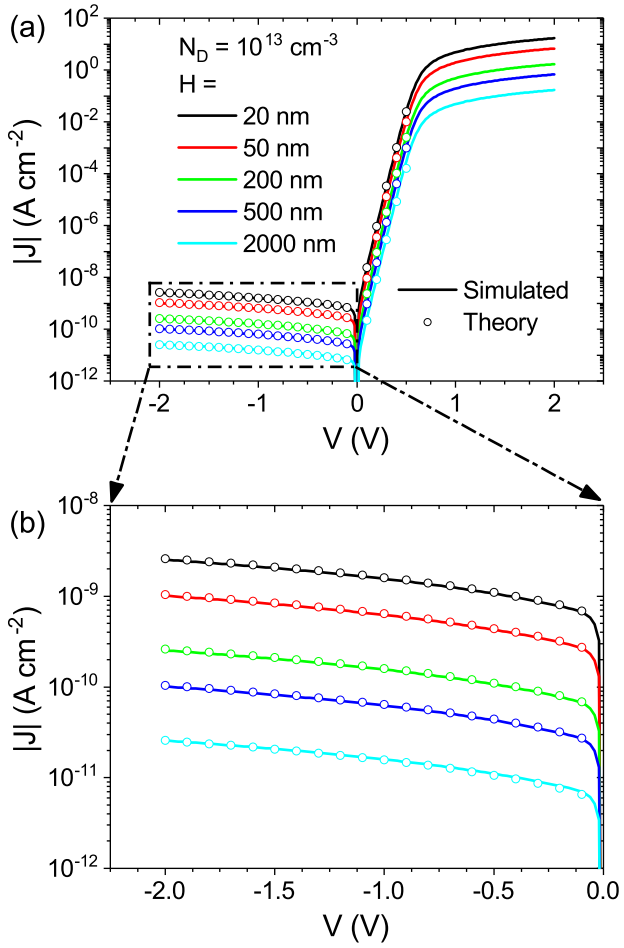

Figure 4: $|J| - V$ characteristics of simulated Schottky diodes (solid lines) with different IGZO thicknesses compared to the diffusion theory for thin-film diodes (circles) as derived in Section 3.2.2. (a) Fitting for $V < \phi_{bi}$. (b) In reverse bias.

As J is directly proportional to $\mathcal{E}_{MT}$, a dependence of the current upon film thickness results, which is not present in standard Schottky diode theory.

To investigate further, the $|J| - V$ characteristics calculated using Eq. 12 are compared to simulated results in Fig. 4. The thickness of IGZO was varied over two orders of magnitude (H = 20, 50, 200, 500 and 2000 nm) and $N_D = 10^{13}$ cm^{-3}. The theory is an excellent fit for all of the different thicknesses when $V < \phi_{bi}$ (in this case $\phi_{bi} = 0.6$ V) and the thickness dependence of the current is clearly reproduced.

The difference between the extracted barrier heights using the thin-film diffusion theory

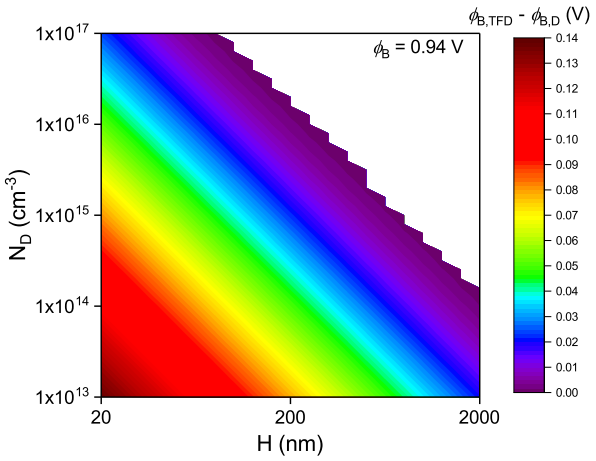

Figure 5: Calculated difference between barrier heights extracted using the thin-film diffusion equation ($\phi_{B,TFD}$) and the standard diffusion equation ($\phi_{B,D}$) for different values of H and N_D. The white region represents values for which the standard depletion approximation applies. The sawtooth shape is a result of the number of data points rather than a real effect.

developed here ($\phi_{B,TFD}$) and standard diffusion theory ($\phi_{B,D}$) can be expressed as

$$\phi_{B,TFD} - \phi_{B,D} = \frac{kT}{q} ln \left[\frac{\mathcal{E}_{MT}(0)}{\mathcal{E}_M(0)} \right]. \tag{13}$$

In Fig. 5, the difference between the two is mapped with respect to H and N_D for $\phi_B = 0.94$ V. The white regions are where the thin-film approximation does not apply i.e. $H > W_D$. In this case, failure to consider the thin-film behaviour can lead to a significant underestimation of barrier height by up to 15%. Such a large error is significant enough on its own, however, these effects are further exacerbated when considered in combination with barrier lowering mechanisms such as IFL.

3.3 Theory of Inhomogeneities in Thin-Film Diodes

In practical devices, disorder at the Schottky interface makes it unrealistic to assume that the barrier height is homogeneous across the whole area of the device.[12,18–20] In this section a theory of inhomogeneities in fully-depleted thin-film Schottky diodes is derived.

3.3.1 Potential

If the Schottky barrier height varies across different regions then:

$$\phi(x, y, 0) = -\phi_B(x, y) = -[\phi_B^0 - \psi(x, y)], \tag{14}$$

where ψ is the difference between the mean Schottky barrier height, ϕ_B^0, and the local Schottky barrier height. Tung treated this perturbation as the potential due to a dipole layer, ϕ_d, with a dipole moment per unit area of $\mathbf{p_A} = 2\epsilon_0\epsilon_s\psi(x, y)\mathbf{k}$,[11,21] thus the dipole potential is

$$\begin{aligned}\phi_d(x, y, z) &= \frac{1}{4\pi\epsilon_0\epsilon_s}\frac{\mathbf{p}\cdot(\mathbf{r}-\mathbf{r}')}{|\mathbf{r}-\mathbf{r}'|^3} \\ &= \int_S \frac{1}{4\pi\epsilon_0\epsilon_s}\frac{\mathbf{p_A}\cdot(\mathbf{r}-\mathbf{r}')}{|\mathbf{r}-\mathbf{r}'|^3}dS \\ &= \int \frac{\psi(x', y')}{2\pi}\frac{z\,dx'dy'}{[z^2 + (x'-x)^2 + (y'-y)^2]^{3/2}}.\end{aligned} \tag{15}$$

Consider the geometry in Fig. 6 where the Schottky junction occurs at the $z = 0$ plane and there is a dipole sheet which is infinite in the y-direction and has a width L_0 in the x-direction, such that the centre of the strip is at $x = 0$. In this case:

$$\phi_B^0 + \psi(x, y) = \begin{cases} \phi_B^0 - \delta & |x| < L_0/2 \\ \phi_B^0 & |x| > L_0/2, \end{cases} \tag{16}$$

where δ is the potential barrier height of the inhomogeneity. The higher barrier regions are ignored as the current passing through them is negligible. Therefore the potential due to the dipole sheet (ϕ_s) is

$$\phi_s(x, y, z) = \frac{\delta}{\pi}\left[\arctan\left(\frac{|x| + \frac{L_0}{2}}{z}\right) - \arctan\left(\frac{|x| - \frac{L_0}{2}}{z}\right)\right]. \tag{17}$$

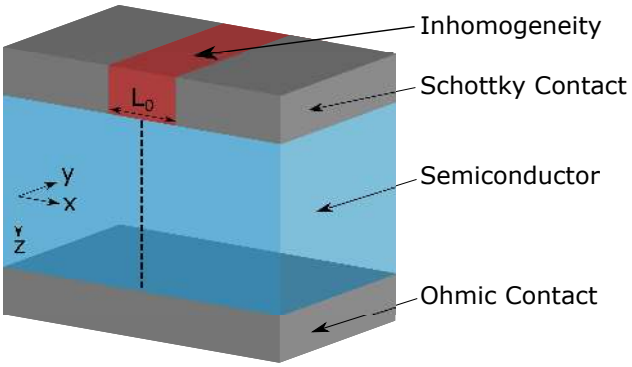

Figure 6: Geometry of the dipole sheet approximation and related simulations for fully depleted thin-film Schottky diodes. The dashed line represents where profiles in Figs. 7, 13 and 14 are taken.

Hence the conduction band minimum is

$$E_C(x,z) = q\phi_B^0 + \frac{q^2 N_D}{2\epsilon_0\epsilon_s}z^2 - q\mathcal{E}_{MT}z - \frac{q\delta}{\pi}\left[\arctan\left(\frac{|x|+\frac{L_0}{2}}{z}\right) - \arctan\left(\frac{|x|-\frac{L_0}{2}}{z}\right)\right], \quad (18)$$

where the centre of the inhomogeneity is at $x = 0$, L_0 is the width of the inhomogeneity and δ is the difference between the mean barrier height, ϕ_B^0, and the barrier height of the inhomogeneity.

Figure 7a shows a comparison of the analytical expression for $E_C(0,z)$ and simulated results for different thicknesses of IGZO (H = 20, 50, 200 and 500 nm). In this case, $\phi_B^0 = 0.94$ V, $L_0 = 10$ nm, $\delta = 0.2$ V, $N_D = 10^{15}$ cm^{-3} and $V = 0$ V. The theory clearly reproduces the saddle points in E_C which are formed for all semiconductor thicknesses except for when $H = 20$ nm. The accuracy of the fitting appears to be reasonable; in all three cases the calculated saddle point energies are found to be within $\pm$ 1% of the simulated values.

The electric field in the semiconductor is

$$\mathcal{E}(x,z) = \frac{qN_D}{\epsilon_0\epsilon_s}z - \mathcal{E}_{MT} + \frac{4\delta L_0(4z^2 - 4x^2 + L_0^2)}{\pi[4z^2 + (2x - L_0)^2][4z^2 + (2x + L_0)^2]}. \quad (19)$$

Figure 7b shows a comparison of the analytical expression for $|\mathcal{E}(0,z)|$ and simulated results

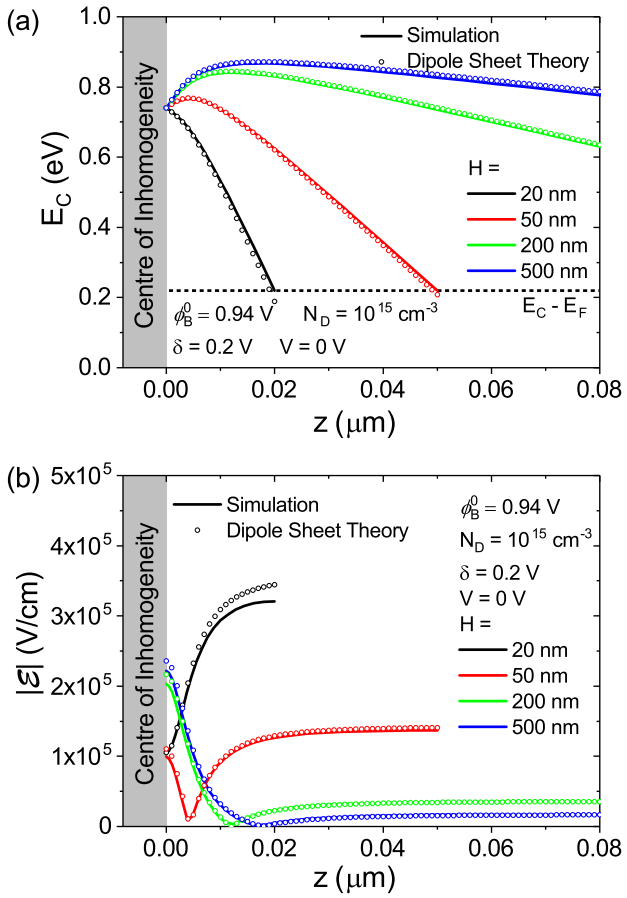

Figure 7: Comparison of the simulation results and the dipole sheet theory for (a) the conduction band minimum in the semiconductor and (b) the magnitude of the electric field in the semiconductor. The profiles shown are for different semiconductor thicknesses directly below the centre of the inhomogeneity ($x = 0$) and near the Schottky interface.

for the same conditions as Fig. 7a. Again, the theory fits the simulations reasonably well, but the quality of the fitting deteriorates as the thickness of the semiconductor layer is reduced. In the 200 and 500 nm cases the fitting on the right hand side of the saddle point is near perfect, but in the 20 nm case the maximum electric field is $\sim 8\%$ higher in the theory (3.45×10^5 V/cm) than the simulation (3.20×10^5 V/cm). Discrepancies like this will invariably have an effect upon the accuracy of any diffusion current theory, but not thermionic emission theory, where the electric field is not taken into account.

The saddle point in E_C only exists under certain circumstances, as demonstrated by Fig. 7a. When the saddle point exists the conduction band minimum must increase with z

from $x = 0$, so

$$\left.\frac{\partial E_C}{\partial z}\right|_{(x,z)=(0,0)} = -q\mathcal{E}_{MT} + \frac{4q\delta}{\pi L_0} > 0, \tag{20}$$

therefore

$$\mathcal{E}_{MT} < \frac{4\delta}{\pi L_0}. \tag{21}$$

Thus, increasing the width of the inhomogeneity and/or reducing δ makes it less likely for a saddle point to form. Moreover, the $\mathcal{E}_{MT}$ dependence suggests that thinner semiconductor layers are less likely to produce a saddle point. Indeed, Eq. 21 further confirms the results of previous experiments and simulations.[13]

The position of the saddle point, z_s, can be calculated using the fact that $\mathcal{E}(0, z_s) = 0$, thus

$$z_s \approx \sqrt{\frac{\delta L_0}{\pi \mathcal{E}_{MT}} - \left(\frac{L_0}{2}\right)^2}, \tag{22}$$

which can be substituted into Eq. 18 to obtain E_{CM}.

3.3.2 Thermionic Emission Current

When the condition for a saddle point to be formed (Eq. 21) is not met, the regions of the Schottky diode with different barrier heights may be modelled as diodes conducting in parallel. Therefore, when thermionic emission is the dominant transport mechanism

$$I = A^* T^2 \exp\left(-\frac{q\phi_B^0}{kT}\right)\left[\exp\left(\frac{qV}{kT}\right) - 1\right]\sum_i A_i \exp\left(\frac{q\delta_i}{kT}\right), \tag{23}$$

which in the case of the single inhomogeneity simulations presented here reduces to

$$I = A^* T^2 \exp\left(-\frac{q\phi_B^0}{kT}\right)\left[\exp\left(\frac{qV}{kT}\right) - 1\right]\left[A_1 + A_2 \exp\left(\frac{q\delta}{kT}\right)\right], \tag{24}$$

where A_1 is the area of the region with barrier height ϕ_B^0 and A_2 is the area of the region with barrier height $\phi_B^0 - \delta$. Importantly, this parallel conduction model does not give rise to

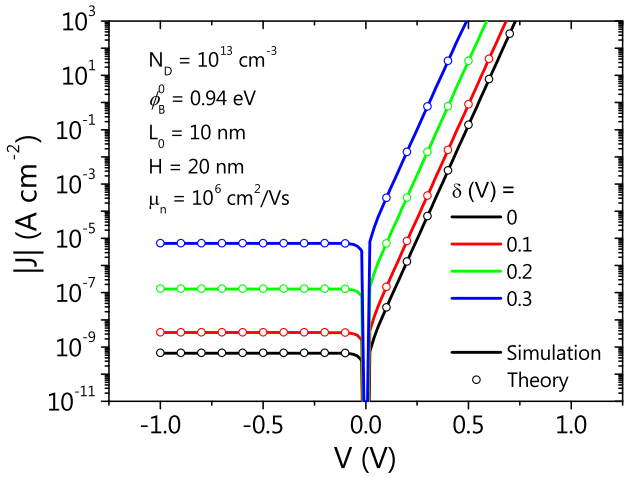

Figure 8: Comparison of simulated and theoretical $|J|$-V characteristics for inhomogeneous Schottky diodes in the absence of a saddle point in E_C. The simulations are thermionic emission limited so the theoretical characteristics are calculated using the thermionic emission parallel conduction theory in Eq. 24. The value of δ is varied from 0 to 0.3 V in 0.1 V increments.

a thickness dependence of the current, as it is only dependent on fixed barrier heights.

The accuracy of the parallel conduction model is displayed in Fig. 8. Both the simulated and calculated $|J|$-V characteristics are plotted for 20 nm thick Schottky diodes with a wide range of δ values. The choice of $\mu_n = 10^6$ cm^2/Vs in the simulation is due to the assumption of infinite mobility in thermionic emission theory.[7] The theory matches the simulation almost perfectly, even for larger values of δ. As there is no saddle point and no IFL is included, the barrier height is independent of bias, leading to a very flat reverse current.

When the saddle point does exist, i.e. Eq. 21 is satisfied, the theory becomes slightly more complex. The analytical expression for E_C is known from Eq. 18, setting $z = z_s$ and expanding the dipole sheet term with respect to x yields

$$E_C(x, z_s) = q\phi_B^0 + \frac{q^2 N_D}{2\epsilon_0 \epsilon_s} z_s^2 - q\mathcal{E}_{MT} z_s - \frac{q\delta}{\pi}\left[2\arctan\left(\frac{L_0}{2z_s}\right) - \frac{16 L_0 z_s}{(L_0^2 + 4z_s^2)^2} x^2 + O(x^4)\right]. \tag{25}$$

This equation approximates how the effective barrier height varies across the whole area

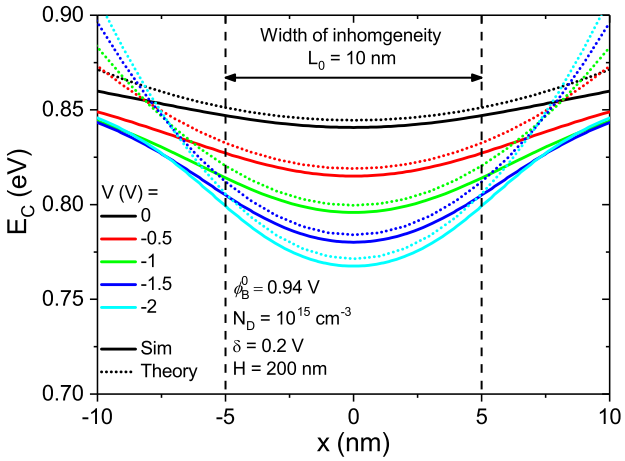

Figure 9: E_C in the x-direction (parallel to the Schottky contact) at the saddle point ($z = z_s$) for five bias points. The solid lines display the simulation results and the dotted lines are values calculated using the expanded version of E_C in Eq. 25.

of the inhomogeneity. Figure 9 shows that the expansion quite accurately reproduces the simulated values of E_C for the region of interest. Importantly, the bias dependence of E_C is also faithfully reproduced. By substituting Eq. 25 into the equation for thermionic emission (Eq. 11) and integrating over the area of the inhomogeneity, the total current through the inhomogeneity, I_{sheet}, can be expressed as

$$I_{sheet} \approx A^* T^2 \frac{\pi L_y (L_0^2 + 4z_s^2)}{4} \sqrt{\frac{kT}{q\delta L_0 z_s}} \exp\left\{ -\frac{q}{kT}\left[\phi_B^0 - \mathcal{E}_{MT} z_s - \frac{2\delta}{\pi}\arctan\left(\frac{L_0}{2z_s}\right)\right]\right\}. \tag{26}$$

From this equation the effective area of the inhomogeneity is

$$A_{eff} = \frac{\pi L_y (L_0^2 + 4z_s^2)}{4} \sqrt{\frac{kT}{q\delta L_0 z_s}} \tag{27}$$

and the effective barrier height for the inhomogeneity is

$$\phi_{B,eff} = \phi_B^0 - \mathcal{E}_{MT} z_s - \frac{2\delta}{\pi}\arctan\left(\frac{L_0}{2z_s}\right). \tag{28}$$

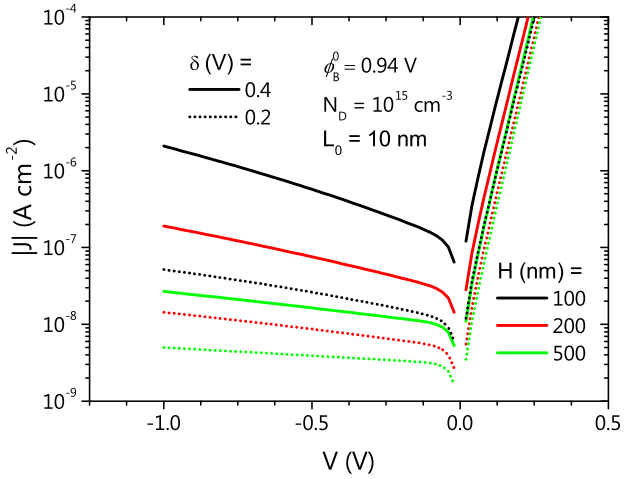

Figure 10: $|J|$-V characteristics for Schottky diodes when a saddle point is present in E_C. The data points are calculated using the thermionic emission theory in Eq. 30. Different values of δ and H are displayed.

By summing over all of the different regions and their respective effective areas and barrier heights the total thermionic emission current is

$$I = A^* T^2 \left[\exp\left(\frac{qV}{kT}\right) - 1 \right] \sum_i A_{effi} \exp\left(\frac{-q\phi_{B,effi}}{kT}\right), \tag{29}$$

which in the case of the simulations presented here becomes

$$I = A^* T^2 \left[A_1 \exp\left(-\frac{q\phi_B^0}{kT}\right) + A_{eff} \exp\left(-\frac{q\phi_{B,eff}}{kT}\right) \right] \left[\exp\left(\frac{qV}{kT}\right) - 1 \right]. \tag{30}$$

The calculated $|J|$-V characteristics for different values of δ and H are shown in Fig. 10. The plots show that the reverse current increases with increasing reverse bias and δ, while reducing as H becomes larger. All of these dependencies are a result of the model capturing the behaviour of the saddle point. The theory reflects this behaviour as the second and third terms in the effective barrier height (Eq. 28). Both terms make a significant contribution to barrier lowering, for example, when $H = 100$ nm, $\delta = 0.2$ V and $V = -1$ V, the second and third terms lower the barrier by 0.06 and 0.12 V, respectively.

When a saddle point is present, a comparison of the theory and simulation is not practical,

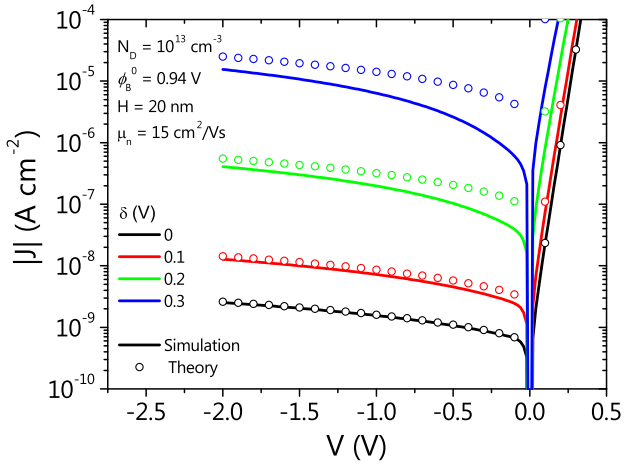

Figure 11: $|J|$-V characteristics of the parallel conduction diffusion theory of thin-film Schottky diodes (Eq. 32) and simulated results for Schottky diodes with different values of δ and a semiconductor thickness of 20 nm.

largely as a result of limitations to the simulation software. Previously, to mimic thermionic emission, the diffusion velocity, v_D, was made significantly larger than the recombination velocity, $v_R \approx \frac{A^*T^2}{qN_C}$. As $v_D \approx \mu_n \mathcal{E}$,[6] this was achieved by setting the mobility to be extremely large e.g. 10^6 cm^2/Vs, as shown in Fig. 8. However, as there is complicated curvature of E_C in the vicinity of the saddle point, the value of v_D cannot be considered to be large in this region. Hence, the simulations cannot be forced into a thermionic emission limit. Despite this limitation, as the model accurately reproduces the behaviour of E_C, the predictions of current are likely sufficiently accurate given the assumptions made for thermionic emission. Moreover, the impossibility of forcing the simulation into a thermionic emission limit indicates the enhanced importance of drift-diffusion in the presence of barrier height inhomogeneities.

3.3.3 Diffusion Current

The previous section focused on the effect of barrier height inhomogeneities upon thermionic emission current. Thermionic emission is a good enough model for semiconductors with high mobilities such as crystalline Si and GaAs,[6] but many emerging semiconductors, including

oxides[22,23] and organics,[24] have far lower mobilities. In addition, and as discussed in the previous section, the curvature of the conduction band in the vicinity of barrier height inhomogeneities reduces the likelihood of thermionic emission being the dominant transport mechanism. Given these factors, the effects of barrier height inhomogeneities upon diffusion current must be considered.

First, consider the case where a saddle point is not present in E_C. In a similar manner to Section 3.3.2, a parallel conduction model based on the thin-film diffusion current (Eq. 12) gives

$$I \approx q\mu_n N_C \exp\left(-\frac{q\phi_B^0}{kT}\right)\left[\exp\left(\frac{qV}{kT}\right)-1\right]\sum_i\left[A_i\mathcal{E}_{MTi}\exp\left(\frac{q\delta_i}{kT}\right)\right]. \tag{31}$$

Hence, for the simulation model used in this section (Fig. 6) the current can be expressed as

$$I \approx q\mu_n N_C\left[A_1\mathcal{E}_{MT1}+A_2\mathcal{E}_{MT2}\exp\left(\frac{q\delta}{kT}\right)\right]\exp\left(-\frac{q\phi_B^0}{kT}\right)\left[\exp\left(\frac{qV}{kT}\right)-1\right] \tag{32}$$

where A_1 is the area and $\mathcal{E}_{MT1}$ is the maximum electric field in the region with barrier height ϕ_B^0 and A_2 is the area and $\mathcal{E}_{MT2}$ is the maximum electric field in the region with barrier height $\phi_B^0-\delta$.

A comparison of the calculated and simulated $|J|$-V curves for different values of δ is shown in Fig. 11. The fitting is not as accurate as the parallel conduction model for thermionic emission, but the theory is increasingly accurate as reverse bias increases. This is because the diffusion current is strongly dependent on the electric field, which is defined by the shape of the conduction band. Despite there being no saddle point present, the E_C beneath the inhomogeneity may still be distorted by the higher barrier regions surrounding it, leading to variations in the true value of $\mathcal{E}_{MT}$ that are not captured by the simplicity of the model. As a result, the simulated current is slightly lower than the current in the model.

When a saddle point is present, developing a theory akin to the one in Section 3.3.2 is more difficult because the current is dependent upon more parameters. When deriving the diffusion

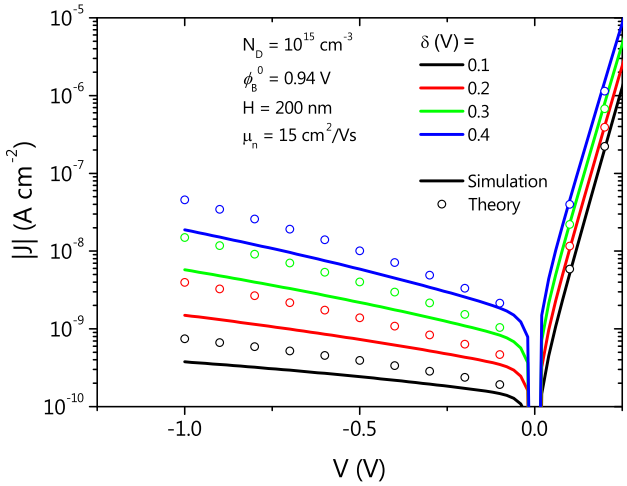

Figure 12: Diffusion limited $|J|$-V characteristics of inhomogeneous thin-film Schottky diodes. Curves compare the theory for when a saddle point in E_C is present (Eq. 36) and simulated results for Schottky diodes with different values of δ and a semiconductor thickness of 200 nm.

current through a diode with a homogeneous barrier height (see Supplementary Information) the current density should be constant throughout the device and J can be removed from the integral (Eq. S3). However, when there is an inhomogeneity in the barrier the problem becomes two-dimensional and the current density becomes inhomogeneous, leading to the following equation:

$$\int_0^H J(x,z)\exp\left\{\frac{q^2N_D}{2\epsilon_0\epsilon_s}z^2 - q\mathcal{E}_{MT}z - \frac{q\delta}{\pi}\left[\arctan\left(\frac{|x|+\frac{L_0}{2}}{z}\right) - \arctan\left(\frac{|x|-\frac{L_0}{2}}{z}\right)\right]\right\}dz$$
$$= qD_nN_C\exp\left(-\frac{q\phi_B}{kT}\right)\left[\exp\left(\frac{qV}{kT}\right)-1\right]. \tag{33}$$

The inclusion of an inhomogeneity in the barrier makes the problem two-dimensional, hence the terms of the integral cannot be separated and the equation cannot be solved analytically.

To overcome the difficultly of formulating a true analytical solution, a modified parallel conduction model was employed. The barrier height of the inhomogeneity is fixed as E_{CM}

(the saddle point energy at $x = 0$) and maximum electric field for this region is set as

$$\mathcal{E}_{MTS} = \frac{E_{CM} - E_N}{H - z_s}, \tag{34}$$

where $E_N = E_C - E_F$ at the interface between the semiconductor and the ohmic contact. This model assumes the electric field is constant between the saddle point and the ohmic contact and that the region between the saddle point and the Schottky contact behaves as an electron sink. Thus, the current can be modelled as

$$I \approx q\mu_n N_C \left[\exp\left(\frac{qV}{kT}\right) - 1 \right] \sum_i \left[A_i \mathcal{E}_{MTi} \exp\left(- \frac{E_{CMi}}{kT} \right) \right]. \tag{35}$$

For the simulations containing a single inhomogeneity this reduces to

$$I \approx q\mu_n N_C \left[\exp\left(\frac{qV}{kT}\right) - 1 \right] \left[A_1 \mathcal{E}_{MT1} \exp\left(- \frac{q\phi_B^0}{kT} \right) + A_2 \mathcal{E}_{MTS} \exp\left(- \frac{E_{CM}}{kT} \right) \right]. \tag{36}$$

Figure 12 displays a fitting of the results for a 200 nm thick semiconductor layer, with $N_D = 10^{15}$ cm^{-3} and a range of δ. The small overestimation of the current can be attributed to two factors. Firstly, the electric field in the theory is higher than the electric field in the simulation due to the curvature of the conduction band near the saddle point. Secondly, the theory assumes that E_{CM} is the barrier height for the whole inhomogeneity, when this is actually a minimum barrier height. Despite these generalisations, the theory reflects behaviour of the simulation quite accurately. Moreover, this represents first time that diffusion theory and inhomogeneities have been considered together. As materials used for thin-film electronics often display significant disorder and mobilities far lower than crystalline Si, the understanding developed here is likely to be of significance to the study of Schottky junctions in thin-film electronics.

3.4 Multiple Inhomogeneities

3.4.1 Potential

In practical devices, there will be many inhomogeneities of varying sizes and magnitudes. To represent this reality analytically, the current must be integrated over the full range of δ and L_0. Such an integration is not possible with the models derived in the previous section, but the model can be further simplified to consider the inhomogeneity as a one-dimensional dipole line, rather than a two dimensional sheet.[11] The potential due to a single dipole line with a dipole moment per unit length of $\mathbf{p_L} = 2\epsilon_0\epsilon_s\delta L_0\mathbf{k}$ can be expressed as

$$\begin{aligned}\phi_l(x,y,z) &= \frac{1}{4\pi\epsilon_0\epsilon_s}\frac{\mathbf{p}\cdot(\mathbf{r}-\mathbf{r}')}{|\mathbf{r}-\mathbf{r}'|^3} \\ &= \frac{1}{4\pi\epsilon_0\epsilon_s}\int_L \frac{\mathbf{p_L}\cdot(\mathbf{r}-\mathbf{r}')}{|\mathbf{r}-\mathbf{r}'|^3}dL \\ &= \int_{-\infty}^{\infty}\frac{\delta L_0 z}{2\pi[x^2+(y'-y)^2+z^2]^{3/2}}dy' \\ &= \frac{\delta L_0 z}{\pi(x^2+z^2)}. \end{aligned} \tag{37}$$

Adding the dipole line term for the inhomogeneity (ϕ_l) to the thin-film potential in Eq. 4 gives

$$\phi(x,z) = -\phi_B^0 - \frac{qN_D}{2\epsilon_0\epsilon_s}z^2 + \mathcal{E}_{MT}z + \frac{\delta L_0 z}{\pi(x^2+z^2)}. \tag{38}$$

Thus, the conduction band minimum is given by

$$E_C(x,z) = q\phi_B^0 + \frac{q^2N_D}{2\epsilon_0\epsilon_s}z^2 - q\mathcal{E}_{MT}z - \frac{q\delta L_0 z}{\pi(x^2+z^2)}. \tag{39}$$

In Fig. 13, the E_C values from Eq. 39 are compared to simulations. Despite the extra simplification, the theory still reproduces the saddle points in E_C, but as the semiconductor thickness is reduced the theory becomes less accurate. The imperfect fitting of E_C for thinner films is a result of the theory tending to negative infinity as z tends to zero, rather than conforming to the boundary conditions of Poisson's equation as outlined in Section 3.1.

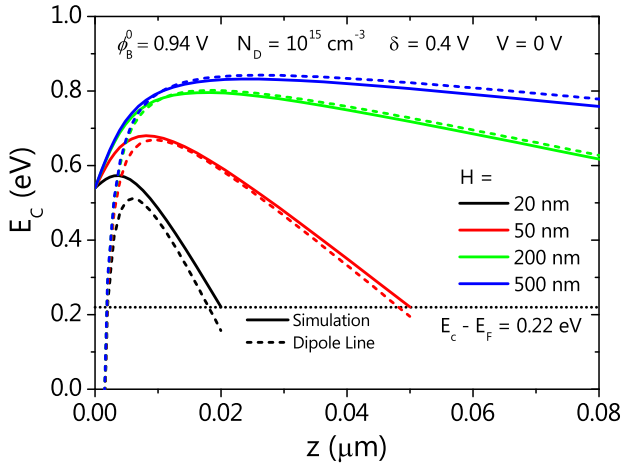

Figure 13: Comparison of simulation results and the dipole line theory for the conduction band minimum of the semiconductor. The profiles shown are for different thicknesses of IGZO directly below the centre of the inhomogeneity ($x = 0$) and near the Schottky interface.

The electric field in the dipole line approximation is given by

$$\mathcal{E}(x,z) = \frac{qN_D}{\epsilon_0\epsilon_s}z - \mathcal{E}_{MT} + \frac{\delta L_0(z^2-x^2)}{\pi\left(z^2+x^2\right)^2}. \tag{40}$$

Hence, at the saddle point $\mathcal{E}(0,z_s) = 0$ so

$$z_s \approx \sqrt{\frac{\delta L_0}{\pi\mathcal{E}_{MT}}}. \tag{41}$$

3.4.2 Thermionic Emission Current

To calculate the current through multiple inhomogeneities, first consider the current through a single inhomogeneity. The conduction band at a distance z_s, the saddle point position, from the Schottky contact is

$$E_C(x,z_s) = q\phi_B^0 + \frac{q^2N_D}{2\epsilon_0\epsilon_s}z_s^2 - q\mathcal{E}_{MT}z_s - \frac{q\delta L_0 z_s}{\pi(x^2+z_s^2)}. \tag{42}$$

Expanding the last term with respect to x yields

$$\frac{q\delta L_0 z_s}{\pi(x^2+z_s^2)} = \frac{q\delta L_0}{\pi z_s\left(1+\frac{x^2}{z_s^2}\right)} \approx \frac{q\delta L_0}{\pi z_s}\left(1-\frac{x^2}{z_s^2}\right), \tag{43}$$

which results in a new approximation for E_C

$$E_C(x,z_s) = q\phi_B^0 + \frac{q^2 N_D}{2\epsilon_0\epsilon_s}z_s^2 - q\mathcal{E}_{MT}z_s - \frac{q\delta L_0}{\pi z_s} + \frac{q\delta L_0 x^2}{\pi z_s^3}. \tag{44}$$

Assuming that the maximum point of E_C occurs at z_s for all x between $-L_0/2$ and $L_0/2$, then $E_C(x,z_s)$ will act as the barrier height for the whole of the low barrier region. Thus, the current through the inhomogeneity can be expressed as

$$\begin{aligned} I_{line} &\approx A^*T^2\int_0^{L_y} dy \exp\left\{-\frac{q}{kT}\left[\phi_B^0 - \mathcal{E}_{MT}z_s - \frac{\delta L_0}{\pi z_s}\right]\right\}\int_{-\infty}^{\infty}\exp\left[-\frac{q\delta L_0 x^2}{\pi kT z_s^3}\right]dx \\ &\approx A^*T^2 L_y\pi\sqrt{\frac{kTz_s^3}{q\delta L_0}}\exp\left\{-\frac{q}{kT}\left[\phi_B^0 - \mathcal{E}_{MT}z_s - \frac{\delta L_0}{\pi z_s}\right]\right\}, \end{aligned} \tag{45}$$

where the limits of integration have been extended to $\pm\,\infty$ to simplify the mathematics. Therefore the effective area is

$$A_{eff} = L_y\pi\sqrt{\frac{kTz_s^3}{q\delta L_0}} \tag{46}$$

and the effective barrier height is

$$\Phi_{B,eff} = q\phi_B^0 - q\mathcal{E}_{MT}z_s - \frac{q\delta L_0}{\pi z_s}. \tag{47}$$

By defining $\theta = \sqrt{\delta L_0}$, the inhomogeneity can be characterised with a single parameter. For a fixed thickness and θ, the effective barrier height, E_{CM} is practically the same regardless

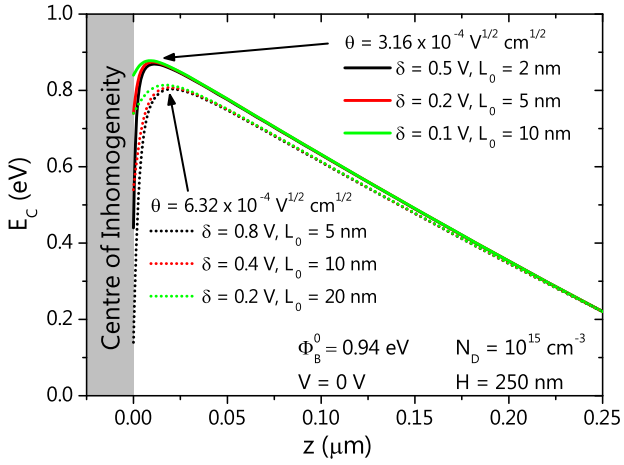

Figure 14: Simulated profile of E_C taken normal to the centre of the inhomogeneity ($x = 0$) in the Schottky contact down to the ohmic contact. Two values of θ are shown, each with three different combinations of δ and L_0.

of the value of δ and L_0, as shown in Fig. 14. Using the new parameter, the effective area can be expressed as

$$A_{eff} = L_y \left[\frac{kT}{q}\right]^{1/2} \left[\frac{\pi}{\mathcal{E}_{MT}^3}\right]^{1/4} \theta^{1/2} \tag{48}$$

and the effective barrier height becomes

$$\Phi_{B,eff} = q\phi_B^0 - 2q\theta\sqrt{\frac{\mathcal{E}_{MT}}{\pi}}. \tag{49}$$

When there is spatial variation of the barrier height, a distribution of θ must be incorporated into the calculation of the current. Such a calculation yields:

$$I = AA^*T^2 \exp\left\{\frac{-q\phi_B^0}{kT}\right\}\left[\exp\left\{\frac{qV}{kT}\right\} - 1\right]\left[1 + \frac{c}{\Gamma\left(\frac{3}{4}\right)L_x}\left[\frac{q\xi^3}{kT}\right]^{1/2}\left[\frac{8\pi}{\mathcal{E}_{MT}}\right]^{1/4} \exp\left(\frac{2q^2\xi^2\mathcal{E}_{MT}}{\pi k^2T^2}\right)\right], \tag{50}$$

where L_x is the width of the diode, c behaves as a quasi-density parameter for low barrier regions, ξ is a measure of the distribution width and Γ is the gamma function. The derivation of Eq. 50 can be found in the Supplementary Information. Using this equation several of

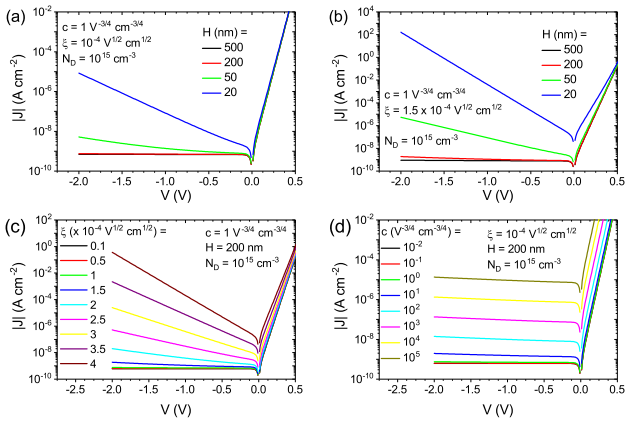

Figure 15: $|J|$-V curves for thermionic emission theory of thin-film Schottky diodes containing a distribution of barrier heights. (a) Different semiconductor thicknesses when $\xi = 10^{-4}$ $\mathrm{V}^{1/2}\mathrm{cm}^{1/2}$. (b) Different semiconductor thicknesses when $\xi = 1.5 \times 10^{-4}$ $\mathrm{V}^{1/2}\mathrm{cm}^{1/2}$. (c) Different values of ξ. (d) Different values of c.

features of inhomogeneous thin-film Schottky diodes can be replicated.[13] In Figs. 15a and b the thickness dependence of the current is recreated, largely due to the current being exponentially dependent upon $\mathcal{E}_{MT}$. Just as in experiments and simulations, the thickness dependence is particularly strong in reverse bias, with the current increasing by many orders of magnitude as thickness is reduced. The reduction of the ideality factor with reducing thickness can also be seen through the reduction of the gradient of the forward current, which is particularly clear in Fig. 15b. A comparison of Figs. 15a and b, also demonstrates that increasing ξ has the effect of increasing sensitivity of the current to the thickness of the semiconductor. Furthermore, Fig. 15c shows that as ξ becomes larger the current increases, as does the bias dependence of the reverse current. Such increases are expected, as ξ reflects the distribution of inhomogeneity magnitudes and sizes. Finally, Fig. 15d shows that once the contribution from the low barrier regions dominates, the current increases linearly with c, a factor which incorporates the density of inhomogeneities.

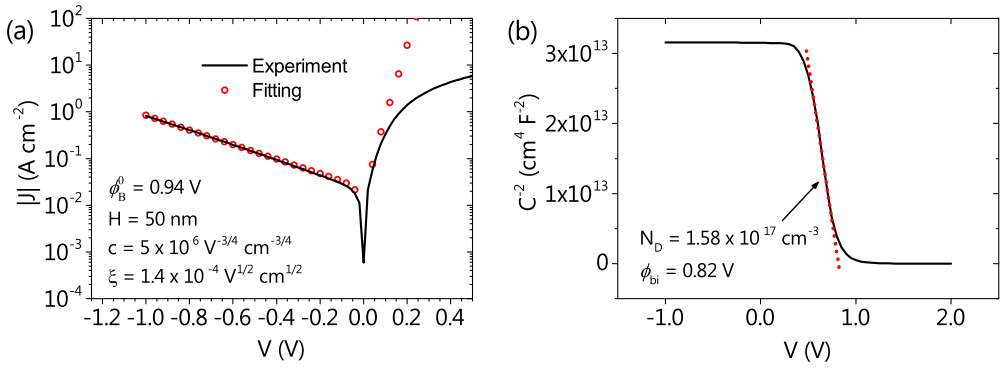

Figure 16: Fitting experimental results. (a) $|J|$-V curves for a 50 nm thick Pd-IGZO Schottky diode fitted with the multiple inhomogeneity theory. Fitting parameters are $\xi = 1.4 \times 10^{-4}$ $\mathrm{V}^{1/2}\mathrm{cm}^{1/2}$ and $c = 5 \times 10^6$ $\mathrm{V}^{-3/4}\mathrm{cm}^{-3/4}$. (b) C^{-2}-V curve used to extract $N_D = 1.58 \times 10^{17}$ cm^{-3} and $\phi_{bi} = 0.82$ V, thus $\phi_B^0 = 0.94$ V is used in the fitting.

3.4.3 Fitting Experimental Results

Pd-IGZO Schottky diodes were fabricated on SiO_2-Si wafers. To form the bottom contact, 3 nm Cr (for adhesion) and 27 nm Pd (for Schottky contact) were deposited via e-beam evaporation. Following the Pd deposition, a 50 nm thick IGZO layer was deposited using radio-frequency sputtering with Ar as the working gas and an IGZO target with a molar ratio of 1:1:2 (In_2O_3:Ga_2O_3:ZnO). Al was chosen as the ohmic contact and was deposited via thermal evaporation and patterned using shadow masks. The J-V properties were measured using an Agilent E5260B semiconductor analyzer and the capacitance-voltage (C-V) measurements were carried out at using an Agilent E4980A LCR meter.

The $|J|$-V curve in Fig. 16a has a high reverse current, which is typical of oxide semiconductor Schottky diodes which have not had oxygen treatment at the Schottky interface.[25] A fitting can be made to the experimental results using $\xi = 1.4 \times 10^{-4}$ $\mathrm{V}^{1/2}\mathrm{cm}^{1/2}$ and $c = 5 \times 10^6 V^{-3/4} cm^{-3/4}$ as fitting parameters. Given that[6]

$$C^{-2} = \frac{2\left(\phi_{bi} - V - \frac{kT}{q}\right)}{q\epsilon_0\epsilon_s N_D}, \tag{51}$$

a linear fitting of the C^{-2}-V curve in Fig. 16b can be used to extract $N_D = 1.58 \times 10^{17}$ cm^{-3}

and $\phi_{bi} = 0.82$ V. By assuming that for IGZO $N_C = 5 \times 10^{18}$ cm^{-3},[15] the barrier height can be estimated as $\phi_B^0 = 0.94$ V. The fitting offers a practical example of how parameters can be extracted using the analytical theory. The quality of the fitting deteriorates under forward-bias as a result of series resistance which is not accounted for in the model.

4 Summary

A theory of homogeneous thin-film Schottky diodes was proposed and was found to emulate the results of device simulations. Equations for the potential within the semiconductor were derived and the effects of image force lowering were calculated. Moreover, the effects of inhomogeneities in thin-film Schottky diodes have been described in an analytical theory for the first time. The thickness dependence of saddle points in the conduction band minimum, previously seen in simulations, was faithfully reproduced by the theory and the saddle point position was accurately predicted. Expressions for the effective barrier height were also calculated and used to derive equations for current transport over an inhomogeneous Schottky barrier. As the transport mechanism may depend on the choice of materials, both thermionic emission and diffusion were considered. An understanding of diffusion-limited transport is especially important for disordered materials, such as those used for thin-film electronics. Current transport across inhomogeneous Schottky barriers was modelled both in the presence and absence of a saddle point in conduction band minimum. When present, the behaviour of the saddle point dominates the current-voltage behaviour of the device. Indeed, though transport via quantum mechanical tunnelling was not considered, the saddle point will play a significant role here too as it determines barrier thickness near the top of the barrier and therefore the transmission of electrons through this region. An equation for thin-film Schottky diodes with multiple inhomogeneities was also derived, which reproduced the trends seen in fabricated thin-film Schottky diodes, including the strong thickness dependence of the reverse current. Finally, an example fitting of a 50 nm thick Pd-IGZO Schottky

diode was demonstrated.

The results presented offer important insight into Schottky junctions in thin-film devices. Clear explanations of the physical phenomena are given in the analytical models and are matched with device simulations. Such analytical theories may be useful for the efficient design of thin-film electronic devices, such as organic light-emitting diodes, as this model offers the correct method for investigating all thin-film interfaces with potential barriers given the correct choice of boundary conditions. The resulting benefit is an improved method for evaluating issues with the interfaces in these devices. Moreover, as focus shifts towards more disordered materials and cost-effective deposition methods, such as printing, barrier inhomogeneities will become more prevalent in electronic devices incorporating Schottky junctions. Indeed, the comprehensive understanding of inhomogeneities developed here may be importance to the development of source-gated transistors, where barrier height inhomogeneities can significantly affect the voltage gain.[14]

Acknowledgement

We are grateful for the technical support from M. McGowen, I. Hawkins, L. Zhang, Yiming Wang and Qian Xin. This work was supported by North-West Nanoscience Doctoral Training Centre, EPSRC grants (EP/N021258/1 and EP/G03737X/1), National Key Research and Development Program of China (2016YFA0301200 and 2016YFA0201800), National Natural Science Foundation of China (11374185 and 11304180).

Supporting Information Available

Supporting Information includes derivations of diffusion current and current through a barrier with multiple inhomogeneities.

References

(1) Jacunski, M. D.; Shur, M. S.; Owusu, A. A.; Ytterdal, T.; Hack, M.; Iniguez, B. A short-channel DC SPICE model for polysilicon thin-film transistors including temperature effects. *IEEE Trans. Electron Devices* **1999**, *46*, 1146–1158.

(2) Valletta, A.; Gaucci, P.; Mariucci, L.; Fortunato, G.; Brotherton, S. Kink effect in short-channel polycrystalline silicon thin-film transistors. *Appl. Phys. Lett.* **2004**, *85*, 3113–3115.

(3) Valletta, A.; Fortunato, G.; Mariucci, L.; Barquinha, P.; Martins, R.; Fortunato, E. Contact effects in amorphous InGaZnO thin film transistors. *J. Display Technol.* **2014**, *10*, 956–961.

(4) Bahubalindruni, P. G.; Kiazadeh, A.; Sacchetti, A.; Martins, J.; Rovisco, A.; Tavares, V. G.; Martins, R.; Fortunato, E.; Barquinha, P. Influence of channel length scaling on InGaZnO TFTs characteristics: unity current-gain cutoff frequency, intrinsic voltage-gain, and on-resistance. *J. Display Technol.* **2016**, *12*, 515–518.

(5) Tung, R. T. The physics and chemistry of the Schottky barrier height. *Applied Physics Reviews* **2014**, *1*, 011304.

(6) Sze, S. M.; Ng, K. K. *Physics of Semiconductor Devices*, 3rd ed.; John Wiley & Sons Inc.: New York, U.S.A., 2006.

(7) Rhoderick, E. H.; Williams, R. H. *Metal-Semiconductor Contacts, Monographs in Electrical and Electronic Engineering No. 19*; Clarendon, Oxford, 1988.

(8) Lee, D. H.; Nomura, K.; Kamiya, T.; Hosono, H. Diffusion-Limited a-IGZO/Pt Schottky Junction Fabricated at 200 on a Flexible Substrate. *IEEE Electron Device Lett.* **2011**, *32*, 1695–1697.

(9) Somvanshi, D.; Jit, S. Mean barrier height and Richardson constant for Pd/ZnO thin film-based Schottky diodes grown on n-Si substrates by thermal evaporation method. *IEEE Electron Device Lett.* **2013**, *34*, 1238–1240.

(10) Singh, R.; Sharma, P.; Khan, M. A.; Garg, V.; Awasthi, V.; Kranti, A.; Mukherjee, S. Investigation of barrier inhomogeneities and interface state density in Au/MgZnO: Ga Schottky contact. *J. Phys. D* **2016**, *49*, 445303.

(11) Tung, R. Electron transport at metal-semiconductor interfaces: General theory. *Phys. Rev. B* **1992**, *45*, 13509.

(12) Werner, J. H.; Güttler, H. H. Barrier inhomogeneities at Schottky contacts. *J. Appl. Phys.* **1991**, *69*, 1522–1533.

(13) Wilson, J.; Zhang, J.; Li, Y.; Wang, Y.; Xin, Q.; Song, A. Influence of interface inhomogeneities in thin-film Schottky diodes. *Appl. Phys. Lett.* **2017**, *111*, 213503.

(14) Zhang, J.; Wilson, J.; Auton, G.; Wang, Y.; Xu, M.; Xin, Q.; Song, A. Extremely high-gain source-gated transistors. *Proceedings of the National Academy of Sciences* **2019**, *116*, 4843–4848.

(15) Fung, T.-C.; Chuang, C.-S.; Chen, C.; Abe, K.; Cottle, R.; Townsend, M.; Kumomi, H.; Kanicki, J. Two-dimensional numerical simulation of radio frequency sputter amorphous In–Ga–Zn–O thin-film transistors. *J. Appl. Phys.* **2009**, *106*, 084511.

(16) Silvaco, Inc., Atlas User's Manual. 2016.

(17) Shannon, J. Thermionic-field emission through silicon Schottky barriers at room temperature. *Solid-State Electron.* **1977**, *20*, 869–872.

(18) Hsu, J.; Manfra, M.; Lang, D.; Richter, S.; Chu, S.; Sergent, A.; Kleiman, R.; Pfeiffer, L.; Molnar, R. Inhomogeneous spatial distribution of reverse bias leakage in GaN Schottky diodes. *Appl. Phys. Lett.* **2001**, *78*, 1685–1687.

(19) Umezawa, H.; Saito, T.; Tokuda, N.; Ogura, M.; Ri, S.-G.; Yoshikawa, H.; Shikata, S.-i. Leakage current analysis of diamond Schottky barrier diode. *Appl. Phys. Lett.* **2007**, *90*, 073506.

(20) Kim, S.-H.; Kim, H.-K.; Seong, T.-Y. Effect of hydrogen peroxide treatment on the characteristics of Pt Schottky contact on n-type ZnO. *Appl. Phys. Lett.* **2005**, *86*, 112101.

(21) Tung, R. Electron transport of inhomogeneous Schottky barriers. *Appl. Phys. Lett.* **1991**, *58*, 2821–2823.

(22) Kamiya, T.; Hosono, H. Material characteristics and applications of transparent amorphous oxide semiconductors. *NPG Asia Mater.* **2010**, *2*, 15–22.

(23) Fortunato, E.; Barquinha, P.; Martins, R. Oxide Semiconductor Thin-Film Transistors: A Review of Recent Advances. *Adv. Mater.* **2012**, *24*, 2945–2986.

(24) Dimitrakopoulos, C. D.; Mascaro, D. J. Organic thin-film transistors: A review of recent advances. *IBM J. Res. Dev.* **2001**, *45*, 11–27.

(25) Mosbacker, H.; Strzhemechny, Y.; White, B.; Smith, P.; Look, D. C.; Reynolds, D.; Litton, C.; Brillson, L. Role of near-surface states in ohmic-Schottky conversion of Au contacts to ZnO. *Appl. Phys. Lett.* **2005**, *87*, 012102.